

## **A numerical study of centre crack under thermo-mechanical load using EFGM**

Mohit Pant<sup>1</sup>, I. V. Singh<sup>1</sup>, B. K. Mishra<sup>1</sup>

### **Summary**

In this work, element free Galerkin method (EFGM) has been used to obtain the solution of centre crack problem under thermo-mechanical loads as it provides a versatile technique to model static as well as moving crack problems without any requirement of re-meshing. Diffraction criterion has been used to model crack geometry. The effect of crack orientation of centre crack has been studied under both mechanical and equivalent thermal loading under plane stress conditions. The values of mode-I and mode-II stress intensity factors have been evaluated by the interaction integral approach.

**keywords:** EFGM, LEFM, centre crack, thermal and mechanical loading, diffraction criteria.

### **Introduction**

Selecting materials and determining the shape and size of different parts of a structure or machine constitute engineering design. In spite of all scientific developments and technological advancements, engineering cannot claim perfection. Imperfections inherent in materials undermine engineering design, often results in catastrophic consequences. Cracks exist in almost all engineering components at macro/micro level. Thermo-mechanical loading may result in either the propagation of pre-existing cracks or may initiate new cracks in the structures. This may finally lead to catastrophic failure of the components resulting in loss of property and lives.

A wide range engineering applications are governed by thermo-mechanical loading. Examples of such applications are piston of an engine, where temperature variation takes place along with mechanical loading, connecting rods of an engine subjected to mechanical as well as thermal loads, damage of solder connections in microelectronic components due to cyclic thermal loading, thermal barrier coatings applied over aero-engine parts, walls of nuclear reactor which are subjected extremely high pressure and temperatures, non-uniform heating of bi-material coatings, ceramic linings in furnaces and vessels used in steel industry where both thermal loading and thermal shock phenomenon takes place, and high temperature pressure vessels and boilers used in industries, etc. Therefore, it has been noticed that the failure of engineering components is not only due to mechanical loads but also due to thermal stresses/thermal fatigue (Lansinger *et al.*, 2007).

---

<sup>1</sup>Department of Mechanical and Industrial Engineering, Indian Institute of Technology, Roorkee 247 667, UA, India, E-mail: iv\_singh@yahoo.com

Thus, the study of crack under thermo-mechanical (Dai *et al.*, 2005) loading is of great importance as it helps us to understand some basic phenomenon such as:

- The effect of micro and macro cracks over the strength of material;
- Direction of crack propagation and crack branching;
- Estimating critical crack length and the safe life period of component;

To model the presence of crack, a number of numerical tools such as finite element method (FEM), boundary element method (BEM) and finite difference method (FDM) are available. Out of these numerical methods, FEM has been found to be the most successful and powerful numerical method for the simulation of fracture mechanics problems. However, FEM is either not suitable or often experiences difficulties in solving a class of problems which require re-meshing and adaptive simulation. The problems which fall in this category are large deformation with element distortion, moving crack simulation, crack growth with arbitrary and complex path, dynamic impact problems, simulation of continuous casting, and breakage of material into large number of fragments, etc. Moreover, the accuracy of the solution depends upon the quality of the mesh in FEM. To handle these difficulties, a new class of methods, known as mesh-free methods (Belytschko and Lu, 1994) has been developed over past ten years. These methods do not require any kind of mesh for the discretization of the problem domain, and only need a set of scattered nodes for construction of an approximation function (Belytschko and Loehnert, 2007). Apart from this, the static crack and crack growth problems have not been analyzed under thermo-mechanical load. Therefore, in the present analysis, element free Galerkin method (Belytschko and Fleming, 1999) has been opted to analyze linear elastic fracture mechanics problems under thermo-mechanical loads. The diffraction criterion (Organ *et al.*, 1996) has been used to model centre crack geometry

### Review of EFGM

In EFGM, the field variable  $u$  is approximated by moving least square approximation (MLS) function  $u^h(\mathbf{x})$  (Belytschko and Lu, 1994), which is given by

$$u^h(\mathbf{x}) = \sum_{j=1}^m p_j(\mathbf{x}) a_j(\mathbf{x}) \equiv \mathbf{p}^T(\mathbf{x}) \mathbf{a}(\mathbf{x}) \quad (1)$$

where,  $\mathbf{p}(\mathbf{x})$  is a vector of basis functions,  $\mathbf{a}(\mathbf{x})$  are unknown coefficients, and  $m$  is the number of terms in the basis.

The unknown coefficients  $\mathbf{a}(\mathbf{x})$  are obtained by minimizing a weighted least square sum of the difference between local approximation,  $u^h(\mathbf{x})$  and field function nodal parameters  $u_I$ . The weighted least square sum  $L(\mathbf{x})$  can be written in the following quadratic form

$$L(\mathbf{x}) = \sum_{I=1}^n w(\mathbf{x} - \mathbf{x}_I) [\mathbf{p}^T(\mathbf{x}) \mathbf{a}(\mathbf{x}) - u_I]^2 \quad (2)$$

where,  $u_I$  is the nodal parameter associated with node  $I$  at  $\mathbf{x}_I$ .  $u_I$  are not the nodal values of  $u^h(\mathbf{x} - \mathbf{x}_I)$  because  $u^h(\mathbf{x})$  is used as an approximant and not an interpolant.  $w(\mathbf{x} - \mathbf{x}_I)$  is the weight function having compact support associated with node  $I$ , and  $n$  is the number of nodes with domain of influence containing the point  $\mathbf{x}$ ,  $w(\mathbf{x} - \mathbf{x}_I) \neq 0$ . By setting  $\partial L / \partial \mathbf{a} = 0$ , a following set of linear equation is obtained as:

$$\mathbf{A}(\mathbf{x})\mathbf{a}(\mathbf{x}) = \mathbf{B}(\mathbf{x})\mathbf{u} \quad (3)$$

By substituting Eq. (3) in Eq. (1), the approximation function is obtained as:

$$u^h(\mathbf{x}) = \sum_{I=1}^n \Phi_I(\mathbf{x})u_I \quad (4)$$

### Problem Formulation

Consider two-dimensional (2D) problem with small displacements on the domain  $\Omega$  bounded by  $\Gamma$ . The governing equilibrium equation is given as:

$$\nabla \cdot \boldsymbol{\sigma} + \mathbf{b} = 0 \text{ in} \quad (5)$$

with the following essential and natural boundary conditions:

$$\mathbf{u} = \bar{\mathbf{u}} \text{ on } \Gamma_u \quad (6)$$

$$\boldsymbol{\sigma} \cdot \bar{\mathbf{n}} = \bar{\mathbf{t}} \text{ on } \Gamma_t \quad (7)$$

where,  $\boldsymbol{\sigma}$  is the stress tensor which is defined as  $\boldsymbol{\sigma} = D(\boldsymbol{\varepsilon} - \boldsymbol{\varepsilon}_T)$ ,  $D$  is the linear elastic material property matrix,  $\boldsymbol{\varepsilon}$  is the strain vector,  $\mathbf{b}$  is the body force vector,  $\mathbf{u}$  is the displacement vector,  $\bar{\mathbf{t}}$  is the traction force and  $\bar{\mathbf{n}}$  is the unit normal,  $\boldsymbol{\varepsilon}_T$  is the thermal strain vector.

For the case of plane stress in an isotropic material with coefficient of thermal expansion  $\beta$  subjected to a temperature change  $\Delta T$ , the thermal strain matrix is given by

$$\boldsymbol{\varepsilon}_T = \begin{Bmatrix} \beta \Delta T \\ \beta \Delta T \\ 0 \end{Bmatrix} \quad (8)$$

Enforcing essential boundary conditions (Krongauz and Belytschko, 1996) using Lagrange multiplier approach (Nguyen *et al.*, 2008) and applying variational principle, the following discrete equations are obtained using Eq. (4):

$$\begin{bmatrix} \mathbf{K} & \mathbf{G} \\ \mathbf{G}^T & 0 \end{bmatrix} \begin{Bmatrix} \mathbf{u} \\ \lambda \end{Bmatrix} = \begin{Bmatrix} \mathbf{f} \\ \mathbf{q} \end{Bmatrix} \quad (9)$$

Where,

$$K_{IJ} = \int_{\Omega} \mathbf{B}_I^T \mathbf{D} \mathbf{B}_J d\Omega,$$

$$f_I = (f_I)_{\text{mech}} + (f_I)_{\text{thermal}},$$

$$(f_I)_{\text{mech}} = \int_{\Gamma_t} \bar{\mathbf{t}} \Phi_I d\Gamma_t,$$

$$(f_I)_{\text{thermal}} = \int_{\Omega} \mathbf{B}_I^T \mathbf{D} \varepsilon_T \Phi_I d\Omega,$$

$$G_{IK} = - \int_{\Gamma_u} \Phi_I \mathbf{N}_K d\Gamma_u, \quad q_K = - \int_{\Gamma_u} \mathbf{N}_K \bar{u} d\Gamma_u,$$

$$\mathbf{B}_I = \begin{bmatrix} \Phi_{I,x} & 0 \\ 0 & \Phi_{I,y} \\ \Phi_{I,y} & \Phi_{I,x} \end{bmatrix}, \quad \mathbf{N}_K = \begin{bmatrix} N_K & 0 \\ 0 & N_K \end{bmatrix}, \quad \mathbf{D} = \frac{E}{1-\nu^2} \begin{bmatrix} 1 & \nu & 0 \\ \nu & 1 & 0 \\ 0 & 0 & (1-\nu)/2 \end{bmatrix}$$

where,  $E$  is modulus of elasticity and  $\nu$  is the Poisson's ratio.

### Results and Discussions

The dimensions of the cracked body used in the present study are taken as  $H = 200$  mm,  $W = 100$  mm and  $2a = 40$  mm as shown in **Fig. 1**. The material selected is ASTM 36 steel (Beer *et al.*, 2002) with modulus of elasticity ( $E$ ) = 200 GPa, Poisson's ratio ( $\nu$ ) = 0.3, far field stress ( $\sigma_o$ ) = 100 MPa, coefficient of thermal expansion ( $\beta$ ) =  $11.7 \times 10^{-6}/^\circ\text{C}$ , Temperature change  $\Delta T = -43.7$  °C. The applied temperature change is such that it produces an equivalent mechanical stress  $E\beta\Delta T = 200 \times 10^3 \times 11.7 \times 10^{-6} \times 43.7 = 99.9$  MPa  $\cong$  100 MPa.

Centre crack problems have been solved to study the effect of crack inclination on stress intensity factors. The centre of crack has been taken at a distance of  $H/2$  i.e. 100 mm from the bottom and  $W/2$  from the edge. To validate the EFGM results, centre crack problem has been solved under mode-I mechanical for  $\alpha=0^\circ$ .

In case of mechanical loading, external far field stress has been applied at two opposite edges of the crack geometry as shown in **Fig. 1a**, whereas in the case of thermal loading, stresses have been developed as a result of temperature change as shown in **Fig. 1b**. Centre crack along with its geometry and boundary conditions is shown in **Fig. 1**. In case of mechanical loading, the bottom edge has been constrained along y-direction, and an external far field stress is applied at the top edge as shown in **Fig. 1a**, whereas in case of thermal loading, both top and bottom edges are constrained along y-direction as shown in **Fig. 1b** and thermal stresses are developed due to change in temperature.

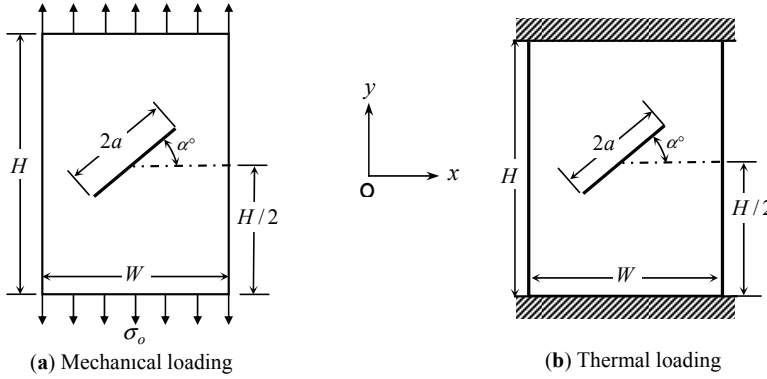


Figure 1: Problem geometries and their dimensions along with boundary conditions

The problem domain has been discretized using 800 nodes along with additional nodes at the crack surface and at the crack tip as shown in **Fig. 2**. A regular nodal distribution has been considered in all simulations. Six point Gauss quadrature (Nguyen *et al.*, 2008) has been used for the numerical integration (Dolbow and Belytschko, 1999) of the Galerkin weak form. A plane stress condition has been assumed. The values of mode-I and mode-II stress intensity factors i.e.  $K_I$  and  $K_{II}$  have been calculated using domain based interaction integral (Dag, 2006; Dolbow and Belytschko, 1998) approach.

### Mechanical Loading

In case of mechanical loading, the results have been obtained for various crack configurations. The length of crack is taken as  $2a=40$  mm. **Fig. 2a** shows a single edge crack configuration subjected to mechanical loading. Both mode-I and mode-II stress intensity factors have been calculated at the crack tip for several values of crack orientation ( $\alpha$ ) as presented in **Fig. 2b**. The maximum value of mode-I stress intensity factor i.e.  $K_I$  is obtained as  $28.5 \text{ MPa}\sqrt{\text{m}}$  at  $\alpha=0^\circ$  (The exact analytical solution (Anderson, 2005) of mode-I stress intensity factor for  $\alpha=0^\circ$  is  $28.7 \text{ MPa}\sqrt{\text{m}}$ ), while the maximum value of mode-II stress intensity factor i.e.  $K_{II}$  is obtained at  $\alpha=40^\circ$ . From the results presented in **Fig. 2b**, it has been noticed that with the increase in  $\alpha$ , the value of  $K_I$  decreases continuously while  $K_{II}$  after attaining its maximum value at  $\alpha=40^\circ$ , starts decreasing as shown in **Fig. 2b**. At  $\alpha=43^\circ$ , the value of  $K_I$  becomes equal to  $K_{II}$  as can be clearly seen from the intersection of both plots in **Fig. 2b**. In order to have a clear visualization of crack tip stress field, the contours of stress component  $\sigma_{yy}$  have been plotted over the specimen geometry. For inclined cracks, two different cases with the inclination of  $0^\circ$  and  $60^\circ$  have been considered as shown in **Fig. 3a & Fig. 3b** respectively. Even with variation of crack inclination the stress field remains symmetrical about the crack line as can be clearly seen from the contour plots.

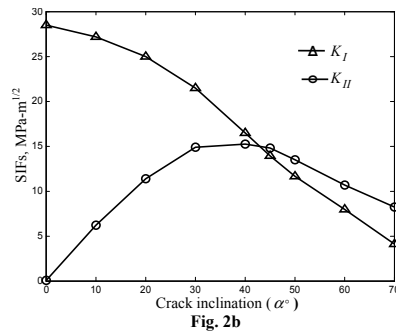
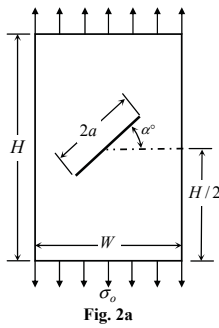


Figure 2: Effect of crack inclination ( $\alpha$ ) on  $K_I$  and  $K_{II}$  of centre crack

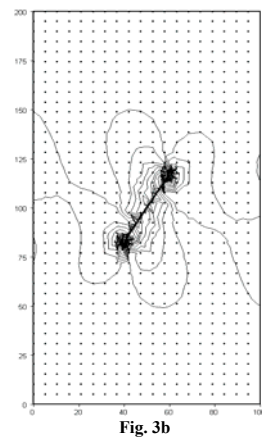
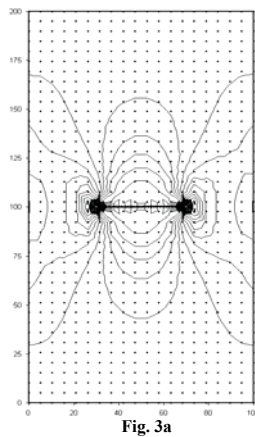


Figure 3: Contour plots of stress ( $\sigma_{yy}$ ) for different inclination subjected to mechanical loading

### Thermal Loading

In case of thermal loading, the results have been obtained with same crack configurations as for mechanical loading. The length of crack is taken as  $2a=40$  mm. **Fig. 4a** shows a centre crack configuration subjected to thermal loading. Both mode-I and mode-II stress intensity factors have been calculated at the crack tip for several values of  $\alpha$  as presented in **Fig. 4b**. The maximum value of  $K_I$  is obtained as  $25.15 \text{ MPa}\sqrt{\text{m}}$  at  $\alpha=0^\circ$ , while the maximum value of  $K_{II}$  is obtained at  $\alpha=40^\circ$ . From the results presented in **Fig. 4b**, it has been noticed that with the increase in  $\alpha$ , the value of  $K_I$  decreases continuously while  $K_{II}$  after attaining its maximum value of  $14.01 \text{ MPa}\sqrt{\text{m}}$  at  $\alpha=40^\circ$  starts decreasing. The contours of stress component  $\sigma_{yy}$  developed due to thermal loading are plotted in **Fig. 5** over the specimen geometry. For inclined cracks, two different values of  $\alpha$  i.e.  $0^\circ$  and  $60^\circ$  have been considered as shown in **Fig. 5a** & **Fig. 5b** respectively. The stress field varies accordingly with crack inclination but remains symmetrical about the length of crack similar to

that in case of mechanical loading. For  $\alpha=0^\circ$ , the value of  $K_I$  is maximum because stresses in y direction dominate at the crack tip. At around  $\alpha=40^\circ$  the values of  $K_I$  and  $K_{II}$  becomes equal which can be clearly seen from intersection of plots in **Fig. 5b**. The variation of mode-I and mode-II stress intensity factor with crack inclination follows the same trend as that of mechanical loading.

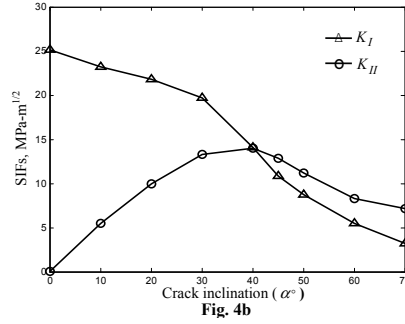
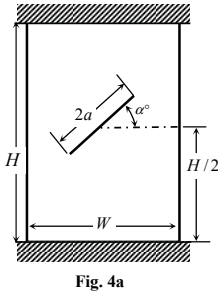


Figure 4: Effect of crack inclination ( $\alpha$ ) on  $K_I$  and  $K_{II}$  of centre crack

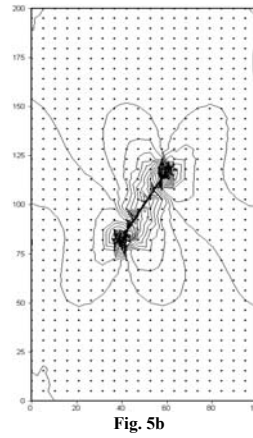
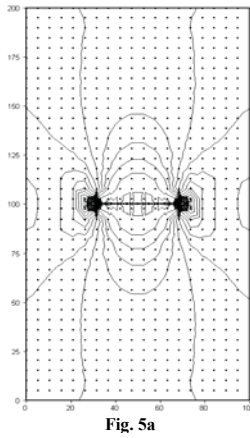


Figure 5: Contour plots of stress ( $\sigma_{yy}$ ) for different inclination subjected to thermal loading

### Conclusions

In the present work, centre crack problem has been solved under thermal as well as mechanical loading condition using EFGM. On the basis of above simulations, it can be predicted that crack inclination has a significant effect over the values of both mode-I and mode-II stress intensity factors. The variation of mode-I and mode-II stress intensity factor with crack inclination under thermal loading follows the same trend as that of mechanical loading. The maximum value of  $K_I$  in case of equivalent thermal loading is about 88% of  $K_I$  for pure mechanical loading. Therefore, it can be concluded that the apart from mechanical load, the thermal

load also plays a major role in the failure of cracked structures.

### References

1. Anderson, T. L., (2005) "Fracture Mechanics Fundamentals and Applications", Taylor and Francis, pp. 52, Boca Raton.
2. Beer, F. P., Johnston, E. R. and Dewolf, J. T., (2002) "Mechanics of Materials", 3<sup>rd</sup> Edition, McGraw-Hill, Singapore.
3. Belytschko, T. and Fleming, M., (1999) "Smoothing, enrichment and contact in the element-free Galerkin method," *Computers and Structures*, 71, pp. 173-195.
4. Belytschko, T. and Loehnert, S., (2007) "Crack shielding and amplification due to multiple micro-cracks interacting with a macrocrack," *International Journal of Fracture*, 145, pp. 1-8.
5. Belytschko, T. and Lu, Y., (1994) "Element-free Galerkin methods, *International Journal for Numerical Methods in Engineering*", 37, pp. 229-256.
6. Dag, S., (2006) "Thermal fracture analysis of orthotropic functionally graded materials using an equivalent domain integral approach", *Engineering Fracture Mechanics*, 73, pp. 2802-2828.
7. Dai, K.Y., Liu, G.R., Han, X. and Lim, K.M., (2005) "Thermo-mechanical analysis of functionally graded material (FGM) plates using element-free Galerkin method", *Computers and Structures*, 83, pp. 1487-1502.
8. Dolbow, J. and Belytschko T., (1998) "An introduction to programming the meshless element free Galerkin method," *Archives of Computational Methods in Engineering*, 5, pp. 207-241.
9. Dolbow, J. and Belytschko, T., (1999) "Numerical integration of Galerkin weak form in meshfree methods", *Computational Mechanics*, 23, pp. 219-230.
10. Krongauz, Y. and Belytschko, T., (1996) "Enforcement of essential boundary conditions in meshless approximations using finite elements", *Computer Methods in Applied Mechanics and Engineering*, 131, pp. 133-145.
11. Lansinger, J., Hansson, T., and Clevfors, O., (2007) "Fatigue crack growth under combined thermal cycling and mechanical loading" *International Journal of Fatigue*, 29, pp. 1383-1390.
12. Nguyen, P., Rabczuk, T., Bordas, S. and Duflot, M., (2008) "Meshless methods: A review and computer implementation aspects", *Mathematics and Computers in Simulation*, 79, pp. 763-813.

13. Organ, D.J., Fleming, M. and Belytschko, T., (1996) "Continuous meshless approximation for non-convex bodies by diffraction and transparency", *Computational Mechanics*, 18, pp. 225-235.

